



Supplementary Materials

Deciphering “Immaturity-Stemness” in Human Epidermal Stem Cells at the Levels of Protein-Coding and Non-Coding Genomes: A Prospective Computational Approach

Tatiana Vinasco-Sandoval ^{1,2,3,†}, Gilles Lemaître ^{2,4,†}, Pascal Soularue ^{1,2}, Michèle T. Martin ^{1,2}
and Nicolas O. Fortunel ^{1,2,*}

¹ Université Paris-Saclay, 91190 Gif-sur-Yvette, France; gloria.vinasco-sandoval@cea.fr (T.V.-S.); pascal.soularue@cea.fr (P.S.); michele.martin@cea.fr (M.T.M.)

² Commissariat à l’Energie Atomique et aux Energies Alternatives (CEA), Laboratoire de Génomique et Radiobiologie de la Kératinopoïèse (LGRK), Institut de Radiobiologie Cellulaire et Moléculaire (iRCM), 2 Rue Gaston Crémieux, 91000 Evry, France; gilles.lemaitre@cea.fr

³ CEA, Institut de Biologie François Jacob (IBFJ), 92265 Fontenay-aux-Roses, France

⁴ Université Paris-Saclay, Univ Evry, 91000 Evry, France

* Correspondence: nicolas.fortunel@cea.fr

† These authors contributed equally to this work.

Supplementary Materials

The following supporting information can be downloaded at:

<https://www.mdpi.com/article/10.3390/ijms25063353/s1>.

Table S1: Sample collection in *KLF4* and *MXD4* studies.

Table S2: Number of enriched terms in individual Over Representation Analysis (ORA).

Table S3: Common differentially expressed lncRNAs identified both in the *KLF4* and in the *MXD4* datasets.

Table S4: ORA selected signature of common differentially expressed protein-coding RNAs identified both in the *KLF4* and in the *MXD4* datasets.

Figure S1: Data preprocessing for the *KLF4* and *MXD4* RNA-seq datasets.

Figure S2: Over representation analysis of common differentially expressed protein-coding RNAs in the *KLF4* and *MXD4* datasets.

Figure S3: Architecture of the computational approach.

Figure S4: Soft thresholding power choice for the *KLF4* and *MXD4* datasets in consensus WGCNA.

Supplementary Tables

Table S1. Sample collection in *KLF4* and *MXD4* studies. Samples corresponding to wild type (WT) and knock-down (KD) cellular contexts.

Model	Sample ID	SRA ID	Cell context
KLF4 (GSE111786)		SRR6829690	
	KLF4_WT1	SRR6829691	WT
		SRR6829692	
		SRR6829693	
	KLF4_WT2	SRR6829694	WT
		SRR6829695	
	KLF4_WT3	SRR6829696	WT
		SRR6829697	
		SRR6829698	
MXD4 (GSE202700)	KLF4_KD1	SRR6829699	KD
		SRR6829700	
		SRR6829701	
	KLF4_KD2	SRR6829702	KD
		SRR6829703	
		SRR6829704	
	KLF4_KD3	SRR6829705	KD
		SRR6829706	
		SRR19165250	WT
	MXD4_WT1	SRR19165251	WT
	MXD4_WT2	SRR19165252	WT
	MXD4_WT3	SRR19165247	KD
	MXD4_KD1	SRR19165248	KD
	MXD4_KD2	SRR19165249	KD
	MXD4_KD3		

Table S2. Number of enriched terms in individual Over Representation Analysis (ORA). Enriched terms were searched based on 2,311 and 5,200 differential expressed protein-coding RNAs for the *KLF4* and *MXD4* datasets, respectively.

Gene set	Enriched terms*	
	<i>KLF4</i>	<i>MXD4</i>
KEGG	27	27
Gene Ontology (GO) – Biological processes	429	353
MSigDB – Hallmarks of genes	12	8
Reactome	27	342
ChEA: ChipX experiment Analysis	37	24
Bioplanet	48	115
Tabula Muris: Single cell transcriptome atlas (<i>Mus musculus</i>)	13	7

* Significant enriched terms after hypergeometric test with ORA (FDR < 0.05).

Table S3 and S4 are available as Excel files

Table S3. Common differentially expressed lncRNAs identified both in the *KLF4* and in the *MXD4* datasets.

Table S4. ORA selected signature of common differentially expressed protein-coding RNAs identified both in the *KLF4* and in the *MXD4* datasets.

Supplementary Figures

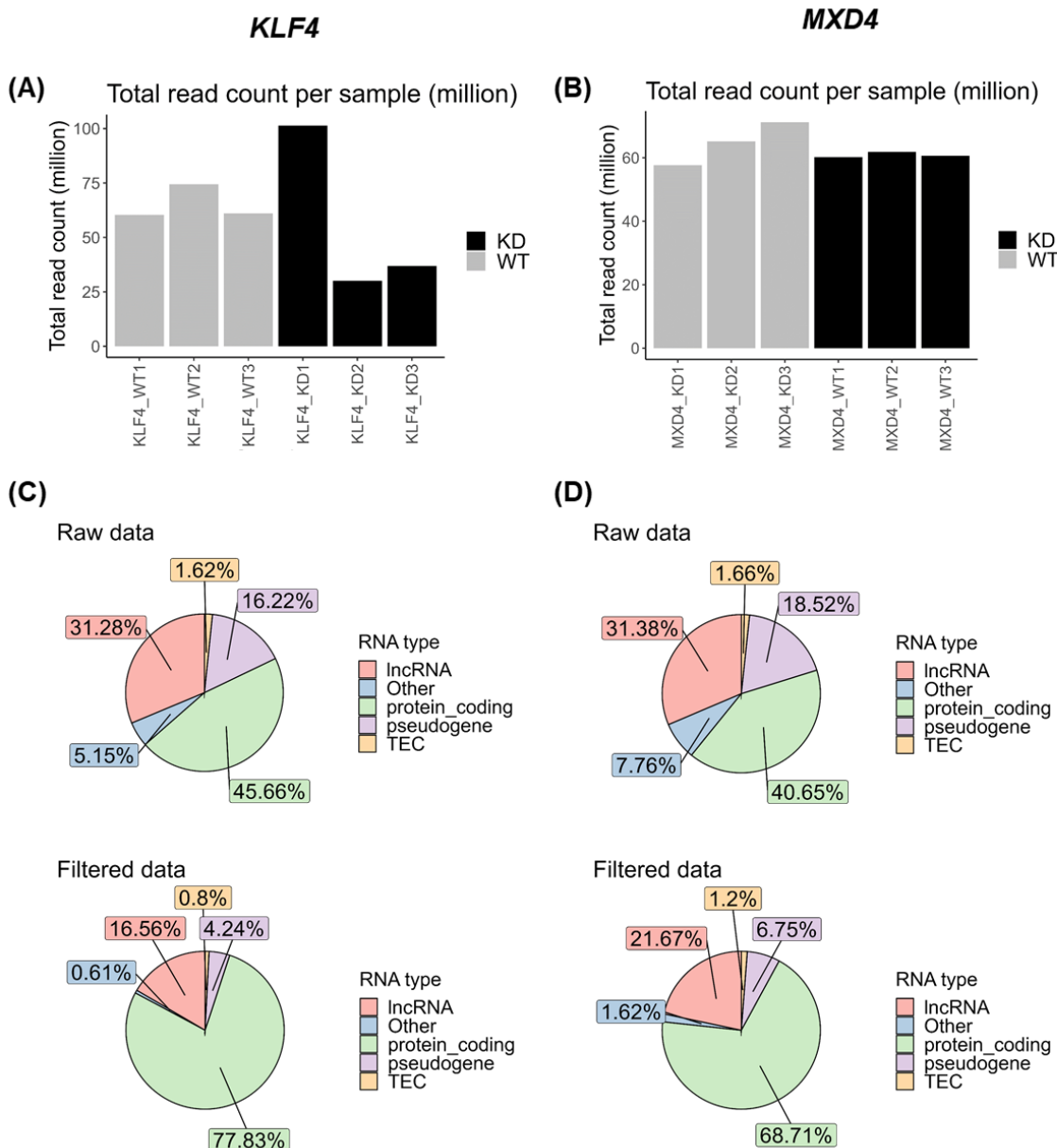


Figure S1. Data preprocessing for the *KLF4* and *MXD4* RNA-seq datasets. **(A-B)** Library size in total million read counts per sample for **(A)** *KLF4* and **(B)** *MXD4* datasets. **(C-D)** RNA species distribution before (Raw data) and after filtering low expressed reads (Filtered data) in both datasets,

(C) KLF4 and (D) MXD4. Other class includes miRNA, misc_RNA, artifact, IG_genes, Mt_rRNA, Mt_tRNA, snoRNA or rRNA.

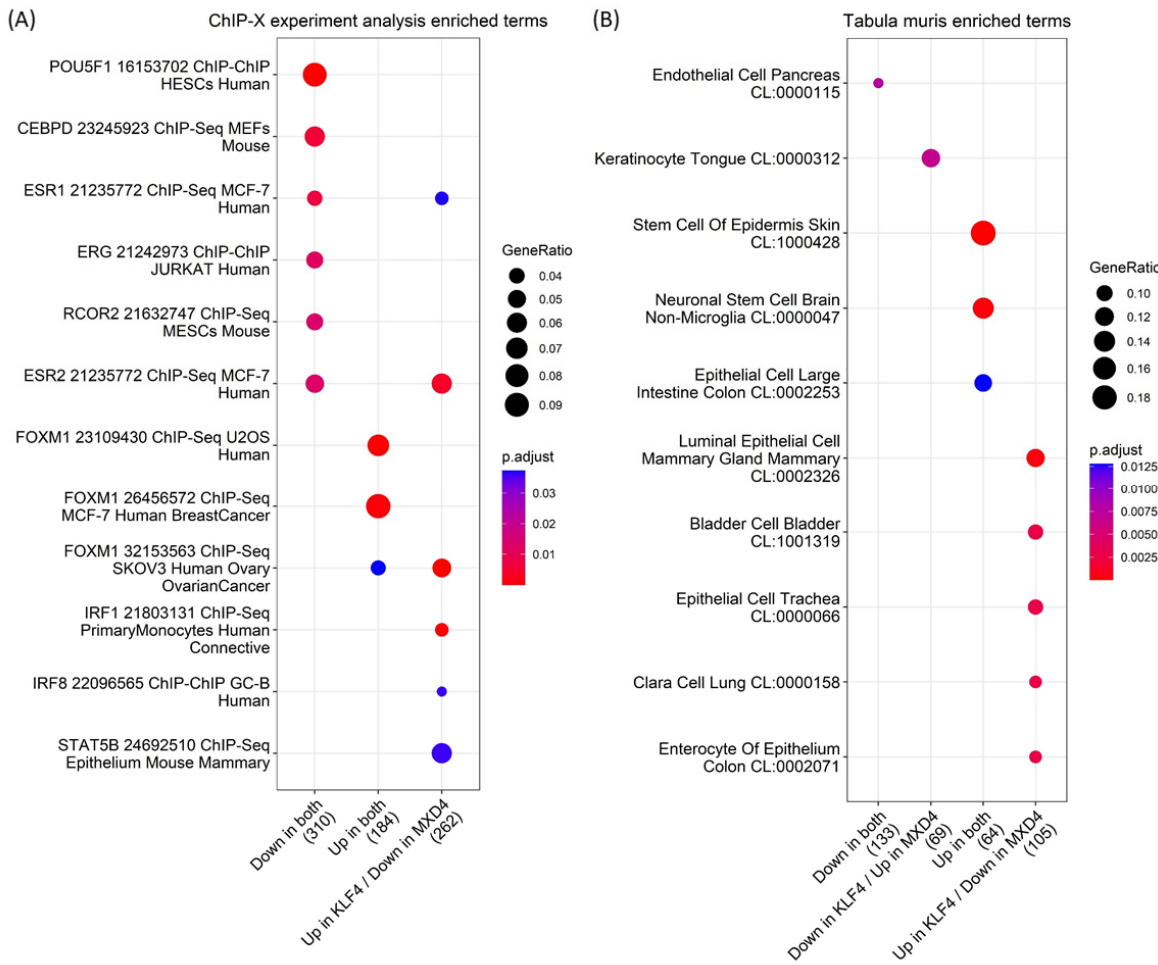


Figure S2. Over representation analysis of common differentially expressed protein-coding RNAs in the KLF4 and MXD4 datasets. Dot plots of enriched terms from (A) ChIP-X experimental analysis and (B) Tabula muris databases. Enrichment was considered significant when False Discovery Rate (FDR) < 0.05.

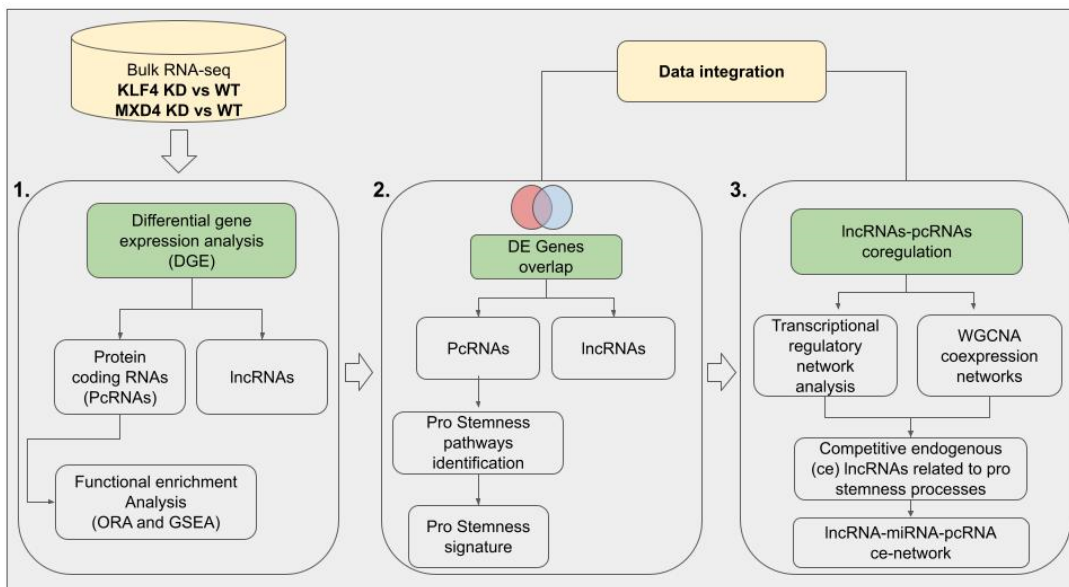


Figure S3. Architecture of the computational approach. Flowchart depicting the main three steps of computational pipeline employed in this study..

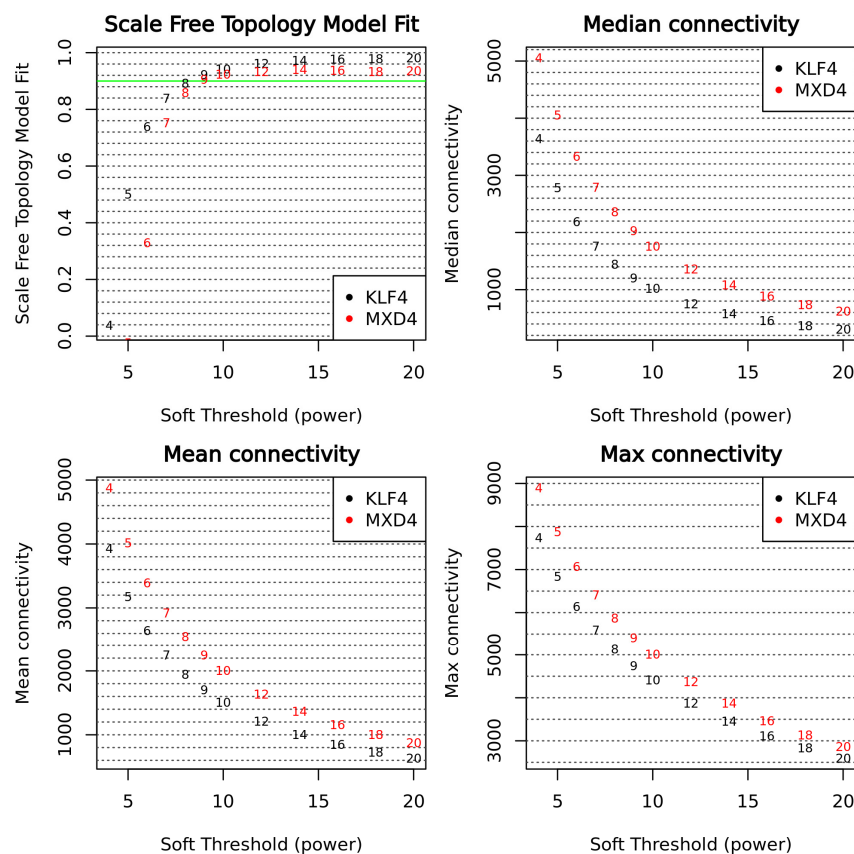


Figure S4. Soft thresholding power choice for the KLF4 and MXD4 datasets in consensus WGCNA. The plots indicate that approximate scale-free topology is attained around the soft-thresholding power of 8 for both models. Numbers inside the plots and x-axes indicate the corresponding soft thresholding powers for network measures (y-axes).